

Eco-Driving Control for Connected Plug-in Hybrid Electric Vehicles in Urban Scenarios with Enhanced Lane Change Engagement

Jie Li¹, Yonggang Liu^{2,*}, Jun Cheng³, Abbas Fotouhi⁴, and Zheng Chen^{5,**}

¹School of Mechanical Engineering, Guangxi University 530004, Nanning, China

²State Key Laboratory of Mechanical Transmission for Advanced Equipment, Chongqing University 400044, Chongqing, China

³Changan Automotive Engineering Institute, 401120, Chongqing China

⁴Advanced Vehicle Engineering Centre, School of Aerospace, Transport and Manufacturing, Cranfield University, Cranfield, Bedfordshire, MK43 0AL, UK

⁵Faculty of Transportation Engineering, Kunming University of Science and Technology, Kunming, 650500, China

* Corresponding Authors: Yonggang Liu (andyliuyg@cqu.edu.cn) and Zheng Chen (chen@kust.edu.cn)

Abstract: Eco-driving control techniques have shown significant potential in reducing energy consumption in urban scenarios. The presence of slow-moving vehicles typically disrupts ecological velocity planning, leading to an increase in energy consumption. To solve it, this study proposes a hierarchical eco-driving control strategy, that integrates speed optimization and lane change decision-making in urban scenarios, to not only ensure traffic efficiency, but also save the energy consumption. Firstly, a data-driven energy model is leveraged in the upper level to estimate the energy consumption of candidate lanes and generate ecological lane change decisions. Then, in the lower level, the preceding vehicles and traffic lights are considered to plan an ecological velocity profile via deep reinforcement learning algorithm after transitions to the target driving lane, thereby enhancing the fuel economy and travel efficiency. A virtual driving environment model is established to verify the proposed method through numerous simulation cases. The results indicate that the proposed method effectively reduces energy consumption while maintaining favorable travel efficiency, compared with conventional benchmarks. Furthermore, the notable improvements are observed particularly in free traffic conditions.

Key Words: Eco-driving; velocity optimization; lane change; deep reinforcement learning; signalized intersection.

I. INTRODUCTION

The persistent increase in number of vehicles has drawn global attention on reducing energy consumption and emissions related to the transportation sector. The rapid development of electrified vehicles as well as connected and automated vehicles (CAVs) presents an expectable opportunity for environmentally-friendly transportation by integrating efficient powertrain systems with intelligent control [1]. Among these techniques, eco-driving control has garnered considerable attention, due to its energy-saving capabilities that has been extensively validated. By accessing and processing complex environmental information, electric CAVs can automatically optimize their motion states by considering the surrounding vehicles, traffic lights and road conditions, which can potentially lead to a remarkably improvement in energy economy and travel efficiency [2].

The primary focus of the eco-driving technology lies in optimizing vehicle driving states, taking into account the characteristics of powertrain system and various driving scenarios. The characteristics of the powertrain system serve as the basis in eco-driving, and the powertrain energy consumption is typically defined as the objective function in the optimal control problem (OCP) of eco-driving. For instance, Wei *et al.* [3] have calculated the hydrogen consumption of a fuel-cell hybrid electric vehicle (HEV) at diverse constant speeds to establish a hydrogen consumption model, which is then leveraged to optimize ecological velocity at signalized intersections. Chen *et al.* [4] have designed a hierarchical eco-driving control method for HEVs, which estimates the working efficiency of the powertrain while optimizing driving speed based on the HEV's driving state. In [5], an energy consumption model is constructed for electric vehicles (EVs) based on neural network, thereby accurately calculating the electricity consumption during velocity optimization. Generally, researches related attempt to consider the characteristics of powertrain systems and precisely calculate energy consumption in a computationally efficient manner [6]. However, for vehicles with hybrid powertrains, such as plug-in hybrid electric vehicles (PHEVs) and fuel-cell hybrid vehicles [7], the energy consumption is quite complicated, since there exist at least two degrees of control freedom.

To now, eco-driving techniques are normally exerted in urban environments. Essentially, it is a typical OCP with the target of promoting energy economy and traffic efficiency, while it is often subjected to some constraints, such as car-following limitation [8], road states [9] and traffic lights [10]. In urban scenarios, to fully promote the eco-driving performance, the signal phase and timing (SPaT) information from traffic lights is suggested to be taken

into account. In this circumstance, eco-driving control methods can optimize the velocity profile to reduce energy consumption and avoid unnecessary stops at signalized intersections. In [11], the optimal driving speed at signalized intersections is solved via dynamic programming (DP), leading to improved fuel economy of internal combustion engine vehicles (ICEVs) while maintaining preferable travel efficiency. To simplify the OCP's complexity, Han *et al.* [12] have assumed the vehicle maintains a constant speed on each route between signalized intersections. On this basis, a green window selector is designed based on the Dijkstra's algorithm, and the optimal time slot is determined through ordinary differential equations. However, the assumption of constant speed on each route may not reflect real-world driving conditions. To address this limitation, a filled-function Pontryagin's minimum principle (PMP) methodology is employed to solve optimal velocity at signalized intersections via forward integration, resulting in significantly improved computational efficiency [13]. Additionally, the flourishing of reinforcement learning (RL) supplies more implementation possibilities for the eco-driving OCP [14]. Wegener *et al.* [15] have proposed an eco-driving controller to plan ecological velocity using the deep deterministic policy gradient (DDPG) algorithm, with SPaT information and preceding vehicles' data serving as the inputs. In another study Li *et al.* [16] have devised a deep reinforcement learning (DRL)-based eco-driving approach at signalized intersections, which employs potential-based shaping functions to enhance the convergence of agent training. In [17], a hybrid DRL-based eco-driving method with long-short term rewards is developed for CAVs at signalized intersections, enabling CAVs to improve driving throughput and energy economy in a mixed traffic environment.

However, most conventional approaches are normally hindered by traffic uncertainties in terms of waiting queues and slow-moving vehicles (SMVs), which can undermine the planned ecological velocity and energy economy [18]. Additionally, signal control, commonly used in intelligent traffic systems to improve traffic efficiency, can also introduce uncertainties to eco-driving control [19]. Since signal control is beyond the scope of this research, it will not be considered in the following discussion. Numerous studies endeavor to address this problem via predicting waiting queues by traffic flow models. For example, Chen *et al.* [20] have proposed a dynamic waiting queue prediction model based on the shockwave theory, and the global speed profile is planned by considering the constraints from the waiting queue. To accurately forecast the length of waiting queues in uncertain traffic environments, Sun *et al.* [21] have established a data-driven traffic flow prediction model to dynamically update waiting queue variations. In addition, the intelligent driver model (IDM) can be leveraged to predict the

influence of waiting the queue. Dong *et al.* [22] have designed a queue discharge method based on the IDM model, in which the ecological velocity is solved using an iterative dynamic programming (IDP) algorithm. Similarly, Liu *et al.* [23] have introduced an eco-driving approach that incorporates the speed limits, SPaT information and queue effects, wherein the release of the queue is predicted based on the IDM model. In [24], the discharge movement of the waiting queue is forecasted by an enhanced queue discharge predictor that takes into account both vehicle and driver dynamics, followed by the solving of velocity profiles by DP and model predictive control (MPC).

Despite advancements in predicting traffic queues, addressing the impact of SMVs remains challenging. Traditional eco-driving methods prioritize optimizing the longitudinal movement of CAVs, which can inevitably reduce the driving speed and travel efficiency due to the presence of SMVs. By incorporating lateral movement into the eco-driving strategies, CAVs can harmonize both the longitudinal and lateral movement, thereby preferably handling traffic uncertainties' influences. The lane change decision-making technologies were firstly investigated in the field of CAVs, by emphasizing both driving safety and travel efficiency [25]. Yao *et al.* [26] have developed a lane-change-aware trajectory optimization model at signalized intersections with considering driving comfort and travel efficiency defined as a joint objective. In another study, Zhao *et al.* [27] have proposed an efficient on-ramp merging strategy for CAVs in multi-lane traffic conditions, and a RL-based controller is established to select a driving lane for CAVs before entering the merging zone. However, the lane change decision methods rarely consider the energy economy in lane change decision-making. Recently, some studies have paid attention to direct promotion of energy economy and travel efficiency via lane change decision-making. For instance, Shunsuke *et al.* [28] have developed an eco-lane selection strategy for CAVs, calculating driving costs for each candidate lane based on cruise speed. Dong *et al.* [29] have proposed a flexible eco-cruising strategy incorporating lane changes, with efficient lane sequencing determined by the Dijkstra algorithm. However, the energy consumption of various candidate lanes is difficult to be precisely estimated, as it is easily influenced by multiple factors, such as planned driving speed, surrounding vehicles and powertrain system of the ego vehicle [30]. In this context, Gu *et al.* [31] have developed a DRL-based eco-driving strategy which integrates optimization of longitudinal motion and lane selection. This strategy takes into account information from the ego vehicle, surrounding vehicles and candidate lanes as inputs. However, few eco-driving strategies have explored the integration of longitudinal and lateral movement on complex urban roads. This is primarily because the presences of traffic lights and preceding vehicles complicates the

estimation of energy consumption for candidate lanes, particularly for PHEVs. In complex urban scenarios, the longitudinal and lateral motion can be influenced by traffic lights, normal human-driven vehicles (HDVs) and SMVs, as shown in Fig 1. In [32], a Markov decision process is utilized to optimize ecological lane selection considering the uncertainties of HDVs, in which the eco-driving OCP is solved by DP in urban scenarios. However, the dynamic variation of the traffic environment makes it intractable to directly optimize lane sequences by traditional optimization algorithms. Furthermore, in urban scenarios, the assumption made by conventional methods that the ego vehicle maintains a constant cruise speed is impractical.

To further advance the eco-driving in urban scenarios and bridge the aforementioned research gaps, a novel eco-driving control strategy is proposed for PHEVs with the lane change engagement. The proposed strategy is designed within a hierarchical framework to enhance eco-driving in complex urban environments, with the aim of improving both energy economy and travel efficiency. In the first layer, the ecological driving lane is determined based on a joint objective, taking into account both energy consumption and travel efficiency. Specifically, energy consumption and travel time are predicted for each candidate lane using a data-driven energy consumption model. In the second layer, longitudinal velocity is optimized by a DRL-based controller considering SPaT information and preceding vehicles. Adequate simulation validations are conducted to analyze the energy economy and adaptivity of the proposed method in-depth. The main contributions of this research can be summarized as follows:

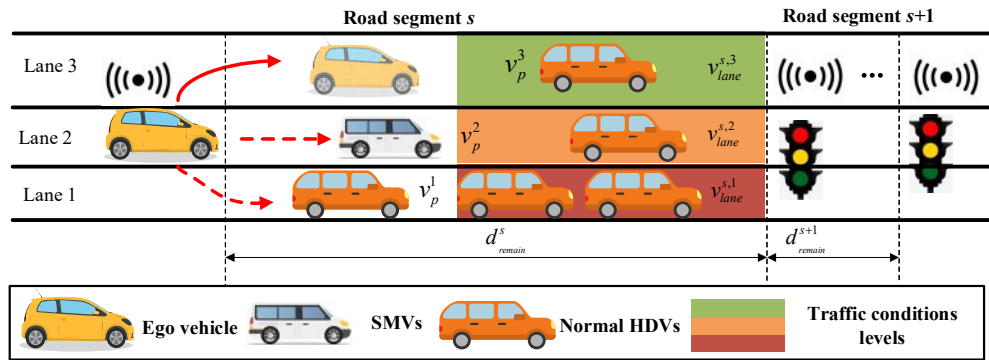


Fig. 1. Illustration of the complex urban scenarios.

1) A novel lane change engagement eco-driving control strategy is proposed for PHEVs, which integrates ecological lateral motion decision-making with longitudinal speed optimization. By coupling longitudinal and lateral motion, the strategy aims to actively optimize the comprehensive driving cost, encompassing energy consumption and travel time. Consequently, it significantly enhances energy economy and travel efficiency under the influence of complex traffic uncertainties.

2) An energy consumption prediction method is developed based on machine learning algorithm to accurately estimate energy consumption for each candidate lane. To derive precise velocity profiles for energy consumption estimation, the method incorporates SPaT information, data from preceding vehicles, and traffic conditions, enabling effective modeling of cruise behaviors and speed variations at the lane level. Furthermore, the characteristics of the PHEV powertrain system are effectively integrated using the machine learning approach.

3) A co-simulation platform is established to validate the performance of the proposed method using simulation of urban mobility (SUMO) and MATLAB software. Numerous simulation cases are conducted in stochastic urban scenarios, featuring multi-lane roads, random HDVs and signalized intersections. The energy economy and adaptability of the proposed method are systematically analyzed and verified across various traffic scenarios.

The remainder of this paper is structured as follows: Section II introduces the construction of the urban scenarios and the ego vehicle, and it formulates the OCP of eco-driving. Section III presents the eco-driving control with lane change decision engagement. The simulation tests are conducted to validate the proposed method in Section IV. Finally, Section V summarizes conclusions and discusses potential future studies.

II. MODELING AND OPTIMAL CONTROL PROBLEM FORMULATION

To explore the eco-driving OCP in complex urban scenarios, this section establishes the environment model and the vehicle kinematic model. Additionally, the OCP formulation for eco-driving in urban scenarios, is presented, which integrates both longitudinal velocity and lateral movement decisions,

A. Urban Scenario Model

A virtual connected environment model is established to investigate eco-driving in complex urban scenarios, and it encompasses multi-lane roads, traffic lights and random HDVs. It is assumed that the ego vehicle can acquire the information in terms of traffic lights, surrounding vehicles and traffic conditions via an intelligent traffic system and sensors. To simulate dynamically varying complex urban scenarios, the SUMO software is utilized to construct the urban scenario model, which has been gradually employed in simulating CAV techniques [33].

The urban scenario model consists of a static road network and dynamic traffic flow. The road network is configured as a three-lane straight road with six signalized intersections. Dynamic traffic flow is generated by a multitude of random HDVs, with their movements simulated using the Krauss model. This motion model calculates a safe velocity considering the current speed and the distance to the preceding vehicle, thereby ensuring driving

safety, especially during emergency stops by the vehicle ahead. The safety constraints can be presented, as:

$$L_e(v_e) + v_e \tau < L_p(v_p) + l_{veh} \quad (1)$$

$$L_e = v_e^2 / 2a_{d\max} \quad (2)$$

$$L_p = v_p^2 / 2a_{d\max} \quad (3)$$

where L_e and L_p are the emergency braking distance at the current speed of the ego vehicle and the preceding vehicle, v_e and v_p represent the driving speed of the ego vehicle and the preceding vehicle, respectively. τ is the reaction time of the driver, l_{veh} denotes the inter-vehicle distance, and $a_{d\max}$ is the maximum deceleration. The safety velocity is calculated, as:

$$v_{safe} = \frac{l_{veh} - v_e \tau}{(v_p + v_e) / 2a_{d\max} + \tau} \quad (4)$$

To ensure that the velocity of HDV complies with dynamic constraints, the desired speed of HDV is calculated based on the speed limit, the safety velocity and the maximum speed within a simulation time step, as:

$$v_{des} = \min[v_{\max}, v_e + a_{\max} t_{step}, v_{safe}] \quad (5)$$

where v_{des} is the desired velocity of the HDV, v_{\max} is the maximum road speed limit, a_{\max} represents the maximum acceleration of the HDV, and t_{step} indicates the simulation time step. To approximate the real-world urban scenarios, HDVs are classified into two types: normal HDVs and SMVs. The normal HDVs' desired velocity varies according to speed limits, whereas the SMVs' desired velocity is set to 10 m/s to simulate the abnormally slow-moving states. Consequently, the established urban scenario model can output four categories of parameters, encompassing ego vehicle, road state, traffic lights and HDVs. These parameters are assumed to be obtained through vehicle-to-everything (V2X) communication and vehicle sensors. The details of these parameters are provided in Table 1. Note that the superscript and subscript in v_{veh}^{lane} indicate the surrounding vehicle's lane position (left, middle or right) and its relation to the ego vehicle (preceding or following).

B. Vehicle Model

The vehicle model in this study encompasses dynamic and powertrain models, which are employed for motion optimization and energy consumption calculation, respectively.

1) Vehicle dynamic models

The vehicle dynamic models include longitudinal and lateral models, of which the former can be established based on Newton's second law, and the longitudinal driving force F_v is calculated, as:

$$F_v = Mgf \cos(\alpha) + \frac{\rho_{air} C_D A v^2}{2} + Mg \sin(\alpha) + \delta M \frac{dv}{dt} \quad (6)$$

where M denotes the vehicle mass, g is the acceleration of gravity, f represents the rolling resistance coefficient, and v is the velocity. ρ_{air} , C_D , A , α and δ are the air density, air drag coefficient, frontal area of vehicle, road grade and correction coefficient of rotating mass, respectively. The longitudinal dynamic state variable, defined as driving distance and velocity, can be calculated by differentiating as follows:

$$\begin{cases} \dot{v} = a \\ \dot{d} = v \end{cases} \quad (7)$$

$$a = \frac{\frac{T_p \eta_t}{r} - F_v}{M \delta} \quad (8)$$

$$T_p = (T_e + T_m) i_t \quad (9)$$

where a is the acceleration, \dot{v} and \dot{d} are the derivative of velocity and driving distance at time domain, respectively. T_p indicates the output torque of the powertrain system, η_t represents the powertrain efficiency, r is the tire radius, i_t indicates the transmission ratio, T_e and T_m are the torque of engine and motor, respectively.

Table 1. The outputs of the urban scenario model

Category	Parameter	Unit	Symbol
Ego vehicle	Velocity of ego vehicle	m/s	v_e
	Position of ego vehicle	m	p_e
	Lane number	-	l_{num}
Road state	Speed limit	m/s	v_{max}
	Traffic flow	veh/h	$q^{s,j}$
	Traffic density	veh/km	$\rho^{s,j}$
Traffic light	Distance to the next traffic light	m	d_{tl}
	Current signal phase	-	st_{tl}
	Remaining time of current phase	s	t_{remain}
Surrounding vehicle	Velocity of preceding vehicle	m/s	v_p
	Inter-vehicle distance to	m	d_p

preceding vehicle		
Velocity of front and rear vehicles on the side lane	m/s	v_{veh}^{lane}
Inter-vehicle distance of front and rear vehicles on the side lane	m	d_{veh}^{lane}

To simulate the lateral motion of ego vehicle, a lateral dynamic model is established with disregarding the extreme slip conditions. The steering process is assumed as an ideal Ackermann steering, and the lateral dynamics are formulated, as:

$$\begin{cases} \dot{d}_x = v \cos \psi \\ \dot{d}_y = v \sin \psi \\ \dot{\psi} = \frac{v \tan \delta}{L_{veh}} \\ v = \sqrt{v_x^2 + v_y^2} \end{cases} \quad (10)$$

where ψ represents the yaw angle, δ is the front wheel steering angle, L_{veh} denotes the length of the vehicle, v_x and v_y are the longitudinal and lateral velocities, d_x and d_y are the longitudinal and lateral positions. The longitudinal velocity is equal to the driving speed when the vehicle is moving forward.

In this study, a PHEV with parallel powertrain is selected as the ego vehicle, as shown in Fig 2. The powertrain system models are established to evaluate the performance of the proposed method, including the engine, motor and the power battery.

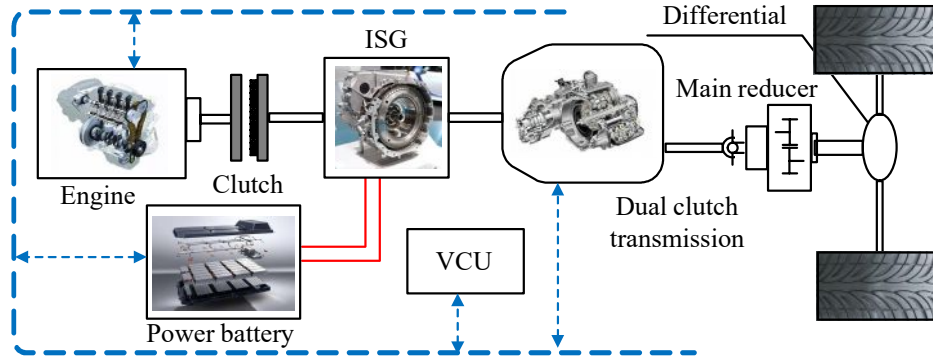


Fig. 2. Powertrain system of the PHEV.

In the eco-driving OCP, the transient characteristics of the engine are normally ignored, and the fuel consumption Q_{fuel} (unit: kg) can be calculated, as:

$$\dot{m}_{fuel} = f_c(T_e, n_e) \quad (11)$$

$$Q_{fuel} = \int \frac{\dot{m}_{fuel} \cdot T_e \cdot n_e}{3.6 \times 10^6 \times 9550 \rho_{fuel}} dt \quad (12)$$

where \dot{m}_{fuel} is the transient fuel consumption rate (unit: g/kwh), f_e is the relationship between fuel consumption and engine working states obtained via calibration experiments, n_e denotes engine rotation speed, ρ_{fuel} represents the fuel density. Similarly, the motor model calculates the working power based on the efficiency map acquiring from calibration experiments, and the motor working power P_m can be formulated, as:

$$\eta_m = f_m(T_m, n_m) \quad (13)$$

$$P_m = \begin{cases} \frac{T_m \cdot n_m}{9550 \eta_m} & T_m > 0 \\ \frac{T_m \cdot n_m \cdot \eta_m}{9550} & T_m < 0 \end{cases} \quad (14)$$

where f_m represents the motor working efficiency map, n_m is the motor rotation speed, and η_m indicates the motor efficiency. In the work, the energy consumption of accessories is neglected. Then, the variation of battery state of charge (SOC) is modelled based on Kichoff's law, as:

$$I_b = \frac{E - \sqrt{E^2 - 4RP_b}}{2R} \quad (15)$$

$$SOC(t) = SOC_0 - \frac{1}{Q_b} \int_0^t I_b(t) dt \quad (16)$$

where I_b , E , R and P_b are the current, open circuit voltage, internal resistance and power of battery, respectively. SOC_0 means the initial SOC, Q_b is the battery capacity. The electricity consumption can be accumulated, as:

$$Q_{ele} = \int \frac{I_b \cdot E}{3.600 \times 10^6} dt \quad (17)$$

C. Optimal Control Problem of Eco-driving

The objective of this eco-driving OCP is to simultaneously optimize the energy economy and travel efficiency in complex urban scenarios. Distinguishing from conventional eco-driving approaches, which merely define acceleration as the control variable, both longitudinal motion and lateral motion decisions are set as control variables in this OCP. For this reason, the ego vehicle is capable of preferably addressing the influence of traffic uncertainties

in complex urban scenarios. The control variables $\mathbf{u} = [a, d_l]^T$ include longitudinal acceleration and lane change decision. Consequently, the state variables are set as $\mathbf{x} = [v, SOC, d, l_{num}]^T$ consist of velocity, battery SOC, driving distance and lane number. In this context, a joint optimization objective is formulated to balance energy economy and travel efficiency time by integrating energy consumption and travel in the time domain, as:

$$J = \int_0^T (\lambda_e E(\mathbf{x}, \mathbf{u}) + \lambda_t T(\mathbf{x}, \mathbf{u})) dt \quad (18)$$

where $E(\mathbf{x}, \mathbf{u})$ represents the energy consumption, $T(\mathbf{x}, \mathbf{u})$ is the travel time, λ_e and λ_t are the coefficients of energy consumption and travel time, respectively. The constraints of this OCP must account for dynamic limitations, powertrain capabilities, speed limits, and initial and final state conditions, which are formulated as follows:

$$\begin{cases} a_{\min} \leq a \leq a_{\max} \\ d_l \in [-1, 0, 1] \\ v_{\min} \leq v \leq v_{\max} \\ v_0 = v_{\text{initial}} \\ d_0 = d_{\text{initial}} \\ T < T_{\max} \\ SOC_{\min} \leq SOC \leq SOC_{\max} \end{cases} \quad (19)$$

where a_{\min} and a_{\max} are the limits of acceleration, v_{\min} and v_{\max} are the limits of velocity, v_{initial} and d_{initial} are the initial value of velocity and driving distance, T_{\max} is the maximum travel time, SOC_{\min} and SOC_{\max} are the limits of SOC. Obviously, the eco-driving OCP in complex urban scenarios is a nonlinear OCP, containing multiple state variables, control variables and constraints. Therefore, conventional optimization algorithms struggle to achieve an optimal control result with high computational efficiency.

III. ECO-DRIVING CONTROL WITH ENHANCED LANE CHANGE DECISION ENGAGEMENT

To address the eco-driving OCP in complex urban scenarios, the proposed method that integrates lane change decision-making and velocity optimization is developed using a hierarchical control framework, as shown in Fig. 3. The eco-driving layer firstly predicts the energy consumption for each candidate lane using a data-driven model. Subsequently, the ecological lane change decision is made considering both energy economy and travel efficiency. Consequently, the ecological velocity is planned using DRL algorithm with fully considering the influence of multiple categories of information after changing to the target lane. By this manner, the proposed eco-driving

approach enables to traffic uncertainties in urban scenarios in a computationally-efficient way.

A. Energy Consumption Prediction at Lane Level

In this study, the ego vehicle is assumed to drive on a flat road, and the energy consumption in each lane is primarily influenced by the driving speed. Hence, accurate estimation of driving states in the candidate lane is crucial for energy consumption prediction. Traditional speed prediction algorithms focus on speed variation in short time domain [34] or long-term cruise profiles generation based on traffic flow [35]. However, these methods are not suitable for energy consumption prediction at the lane level. To precisely predict energy consumption in candidate lanes, a velocity profile generation method is designed, combining traffic flow and speed variations.

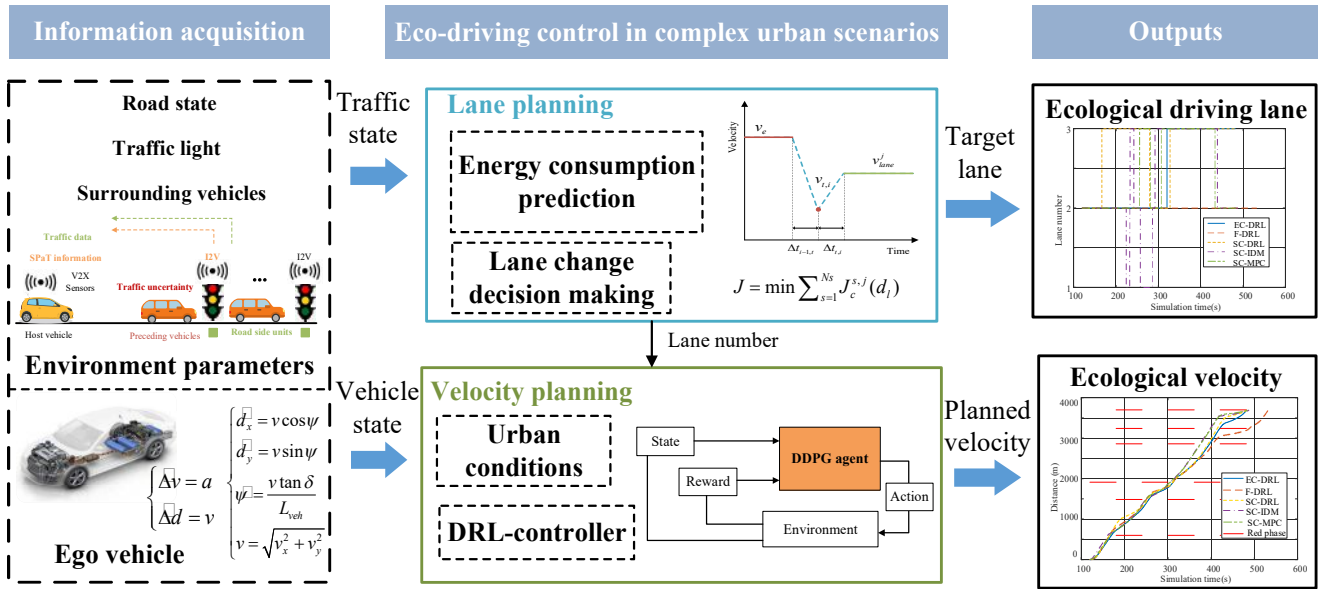


Fig. 3. Schematic of eco-driving control system in urban scenarios considering traffic uncertainties

The driving path is divided into numerous road segments according to the position of the traffic lights. Consequently, the steady velocity at the lane level is influenced by the preceding vehicles and traffic flow. Assuming that the preceding vehicle's speed and the traffic flow remain constant in a short time horizon, the steady velocity in the candidate lane can be formulated by considering traffic conditions, preceding vehicles and target velocity, as:

$$v_{lane}^{s,j} = \begin{cases} v_{traff}^{s,j} = \frac{q^{s,j}}{\rho^{s,j}} & \text{if } v_{traff}^{s,j} < v_p \\ v_p & \text{if } v_p \leq v_{traff}^{s,j} \\ v_e^{tar} & \text{if } v_e^{tar} \leq \min(v_{traff}^{s,j}, v_p) \end{cases} \quad (20)$$

where $v_{lane}^{s,j}$ is the steady velocity in the candidate lane, s and j mean the number of road segment and lane,

respectively. $v_{traff}^{s,j}$ represents the effective velocity of the road segment, $q^{s,j}$ and $\rho^{s,j}$ are the traffic flow and density. The effective velocity is calculated based on shockwave theory [36]. v_p denotes the velocity of the preceding vehicle, v_e^{tar} is the target velocity of the ego vehicle. The lane steady velocity only reflects the cruise states, whereas the velocity variations can lead to extra energy consumption when ego vehicle's velocity differs from the lane steady velocity. To efficiently simulate the velocity variation, this process is divided into cruising and acceleration/deceleration stages [37], as shown in Fig. 4. It can be observed that the velocity variation process can be determined based on the transition speed $v_{t,i}$ when both the ego vehicle velocity and the lane steady velocity are established. The acceleration during velocity variation is assumed to be constant, and the transition speed can be formulated, as:

$$v_{t,i} = \xi \frac{v_e + v_{lane}^{s,j}}{2} \quad (21)$$

where ξ is the coefficient of velocity variation, which ranges from 0 to 1, is determined empirically [38]. In this study, the coefficient is determined through iterative experiments based on the velocity optimization method introduced later. The specific value is detailed in the Simulation section. The initial time of velocity variation is set to zero, and the velocity profile during the deceleration and acceleration stages can be determined, as:

$$v_i(t) = \begin{cases} v_e + \text{sign}(v_{t,i} - v_e) \cdot a_t & t \in [0, \Delta t_{i-1,t}] \\ v_{t,i} + \text{sign}(v_{lane}^{s,j} - v_{t,i}) \cdot a_t (t - \Delta t_{i-1,t}) & t \in [\Delta t_{i-1,t}, \Delta t_i] \end{cases} \quad (22)$$

$$\Delta t_i = \Delta t_{i-1,t} + \Delta t_{t,i} \quad (23)$$

$$\begin{cases} \Delta t_{i-1,t} = \frac{|v_{t,i} - v_e|}{a_t} \\ \Delta t_{t,i} = \frac{|v_{lane}^{s,j} - v_{t,i}|}{a_t} \end{cases} \quad (24)$$

where a_t is the acceleration during the velocity variation, Δt_i means the duration of the velocity variation. $\Delta t_{i-1,t}$ and $\Delta t_{t,i}$ are the duration of the deceleration and acceleration stages, respectively.

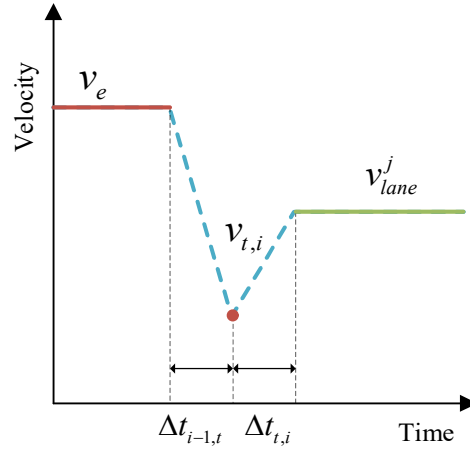


Fig. 4. A synthetic speed profile between two steady speeds

Following the velocity variation process, the ego vehicle's velocity will match the lane's steady velocity, resulting in the presentation of the driving distance and the duration of the cruising process, i.e.,

$$d_{trans}^{s,j} = \int_0^{\Delta t_{i-1,t}} v_i(t) dt + \int_0^{\Delta t_{t,i}} v_i(t) dt \quad (25)$$

$$d_{cruise}^{s,j} = d_{remain}^{s,j} - d_{trans}^{s,j} \quad (26)$$

$$t_{cruise}^{s,j} = d_{cruise}^{s,j} / v_{lane}^{s,j} \quad (27)$$

where $d_{trans}^{s,j}$ and $d_{cruise}^{s,j}$ represent the driving distance of the velocity variation and the cruise process, $d_{remain}^{s,j}$ is the remaining distance in the current road segment, $t_{cruise}^{s,j}$ is the duration of the cruise process. The energy consumption in the candidate lane can be calculated via integration in the time domain. Instantaneous energy consumption cost is estimated using a data-driven model based on back propagation neural network. This model defines velocity, acceleration and SOC of the PHEV as the inputs: $\hat{c}ost_{energy} = f_{NNC}(v, a, SOC)$. The powertrain energy consumption cost can be accurately estimated via this data-driven model, and further details of this model are presented in [6]. Based on equations (20) to (27), the duration and velocity profile of the cruise process, as well as the velocity variations, can be determined. Consequently, the energy consumption can be predicted through time-domain integration, as:

$$\hat{c}ost_e^{s,j} = \int_0^{\Delta t_i} f_{NNC}(v_i(t), a_i(t), SOC) dt + \int_0^{t_{cruise}} f_{NNC}(v_{lane}^j, 0, SOC) dt \quad (28)$$

where $\hat{c}ost_e^{s,j}$ is the predicted energy consumption cost in the j th lane, f_{NNC} is the data-driven energy consumption model. Consequently, the energy consumption in each candidate lane can be predicted based on the information

from V2X communication and sensors.

B. Ecological Lane Change Decision-Making Strategy

An ecological lane change decision-making strategy is proposed here to simultaneously improve both energy economy and travel efficiency. Different indexes are designed for energy economy, travel efficiency and driving safety to achieve the objectives and fulfil safety constraints.

1) Comprehensive index of energy economy and travel efficiency

The energy consumption is directly related to the driving speed, enabling the ego vehicle tends to plan lower velocities to reduce energy consumption, potentially deteriorating travel efficiency. Therefore, a unified index is required to evaluate both the performance of energy economy and travel efficiency effectively. Given that the energy consumption has been transformed into energy consumption cost, a comprehensive index is designed to integrate both energy economy and travel efficiency into a unified driving cost, as:

$$J_{cc}^s = c\hat{ost}_e^{s,j} + cost_t^{s,j} \quad (29)$$

$$cost_t^{s,j} = \left(\frac{|v_{t,i} - v_e| + |v_{lane}^{s,j} - v_{t,i}|}{a_t} + \frac{d_{cruise}^{s,j}}{v_{lane}^{s,j}} \right) \zeta_t \quad (30)$$

where J_{cc}^s is the unified driving cost, $cost_t^{s,j}$ is the travel time cost related to travel efficiency, ζ_t represents the transfer coefficient of the travel time to the driving cost (unit: CNY/hour). Similar to energy consumption cost, the travel time cost for each lane is determined by the duration of the cruise and velocity variation processes. The energy consumption is calculated by (28).

2) Safety constraints for lane change

Driving safety constitutes the fundamental constraint of lane change decisions, and the lane change risks mainly come from the preceding and rear vehicles in the target lane. Therefore, the safety constraints for lane changes take into account both the preceding and rear vehicles in the candidate lane to calculate the safe inter-vehicle distance. The safe inter-vehicle distance is calculated based on the desired inter-vehicle distance defined in the IDM model, as:

$$s^* = s_0 + T_0 \cdot v(t) + \frac{v(t) \cdot \Delta v(t)}{2\sqrt{a_{\max} b}} \quad (31)$$

where s_0 is the minimum inter-vehicle distance, T_0 is the constant time headway, $\Delta v(t)$ represents the velocity deviation from the preceding or rear vehicles, b is the desired deceleration. The lane change strategy only issues a lane change decision when the inter-vehicles distance meets the safety constraint. Additionally, a penalty for frequent lane changes is designed to enhance safety and energy economy. The lane change penalty J_c^{lc} is formulated, as:

$$J_c^{lc} = \lambda_{lc} \frac{v_e}{\Delta t_{lc}} \quad (32)$$

where λ_{lc} is the weight factor of the lane change penalty, Δt_{lc} is the time interval since the last lane change. This penalty is influenced by both the velocity and the time interval between changing lanes. The ego vehicle is more inclined to change lanes at lower velocities and after longer time intervals between lane changes to ensure safety. Based on the aforementioned indexes, the comprehensive driving costs for various lanes can be presented, as:

$$J_c^{s,j} = \begin{cases} c\hat{ost}_e^{s,j}(a, v_e, v_{lane}^j, L_{equ}) + cost_t^s(d_{remain}^{s,j}, v_{lane}^j, a_t) + \lambda_{lc} \frac{v_e}{\Delta t_{lc}} & j \neq l_{num} \\ c\hat{ost}_e^{s,j}(a, v_e, v_{lane}^j, L_{equ}) + cost_t^s(d_{remain}^{s,j}, v_{lane}^j, a_t) & j = l_{num} \end{cases} \quad (33)$$

The comprehensive driving cost of candidate lanes is calculated based on the ego vehicle's velocity, target velocity and traffic conditions of the candidate lanes. This approach preferably integrates lateral motion decisions with longitudinal speed. Consequently, the OCP of lane change decision-making is presented, as:

$$J = \min \sum_{s=1}^{Ns} J_c^{s,j}(d_l) \quad (34)$$

$$\text{s.t.} = \begin{cases} d_l \in [-1, 0, 1] \\ \Delta l_p^j \geq s^* \\ \Delta l_f^j \geq s^* \end{cases} \quad (35)$$

where Δl_p^j and Δl_f^j denote the inter-vehicle distance between the preceding and rear vehicles in various lanes. A motivation model is utilized to determine lane change decisions based on the theory of minimizing overall braking induced by the lane change (MOBIL) [39], as:

$$u_{lc} = \frac{J_c^{s,l_c} - J_c^{s,l_a}}{J_c^{s,l_c}} > \Delta J_c \quad (36)$$

where ΔJ_c represents the threshold for imitating lane changes, u_{lc} is the lane change trigger, $J_c^{s,lc}$ and $J_c^{s,ld}$ are the comprehensive driving cost of the current lane and the candidate lane, respectively. The lane change decision is issued when the MOBIL trigger and safety constraints are satisfied. In the proceeding of lane change, a cubic polynomial function is leveraged to generate the velocity trajectory of the lane change process, ensuring continuous acceleration and satisfactory computational efficiency [40].

C. Ecological Longitudinal Velocity Optimization

Drawing from the guide of lane change decision-making strategy, the target longitudinal velocity is optimized considering the influence of both SPaT information and traffic conditions within the road segment. To solve the OCP of ecological velocity, a DRL algorithm is employed to adaptively plan ecological velocity. Various DRL algorithms, including DDPG, proximal policy optimization (PPO) and trust region policy optimization (TRPO), have been utilized in velocity planning. The key considerations in selecting a DRL algorithm are primarily the action space and convergence performance. A continuous action space is essential for effective longitudinal velocity planning in eco-driving control. Previous study has demonstrated that the DDPG algorithm effectively plan continuous velocity profiles at intersections [41]. In this context, the DDPG algorithm is leveraged to derive optimal target velocity, generating continuous acceleration decisions and smooth velocity profiles. The acceleration is set as the action variable, whereas the state variables are the ego vehicle's velocity v , the ego vehicle's acceleration a , velocity deviation Δv , velocity deviation integral Δv_{inte} and derivative $\Delta v'$, respectively. The velocity deviation indicates the difference between the ego vehicle velocity and the green wave speed, which is calculated to avoid unnecessary stops at signalized intersections. The green wave speed is determined via SPaT information, as:

$$v_{gws} = \max(f_{gws} \cdot v_{gws_max}, 1.1 \cdot v_{gws_min}) \quad (37)$$

$$v_{gws_max} = \begin{cases} v_{max}, & st_{il} = green \\ \min(\frac{d_{il}}{t_{remain}}, v_{max}), & st_{il} = red \end{cases} \quad (38)$$

$$v_{gws_min} = \begin{cases} \max(\frac{d_{il}}{t_{remain}}, v_{min}), & st_{il} = green \\ \max(\frac{d_{il}}{t_{remain} + t_{green}}, v_{min}), & st_{il} = red \end{cases} \quad (39)$$

where v_{gws} is the green wave speed, v_{gws_max} and v_{gws_min} are the limits of green wave speed. In addition, v_{min} , st_{il} , d_{il} , t_{remain} and t_{green} are the minimum velocity of road, the state of traffic light, the distance to next traffic light, the remaining time of traffic light and the duration of green phase. Finally, f_{gws} is the coefficient used to adjust green wave speed.

To incentivize the agent simultaneously optimize energy consumption and travel efficiency, a reward function is designed for training, integrating elements of energy economy, travel efficiency and driving safety. It should be noted that an emergency braking policy and a car-following strategy [42] are employed to prevent collisions, which are not included as components of the reward function. The energy economy reward component is formulated, as:

$$r_e = -f_e \cdot f_{NNC}(v, a, SOC) - f_a \cdot a^2 \quad (40)$$

where f_e and f_a are the weight factors. Notably, this element is constructed from penalties of energy consumption and acceleration. The quadratic acceleration penalty is introduced to mitigate extreme accelerations and improve driving comfort. The reward elements corresponding to travel efficiency are consisted of penalty and positive awards. The penalty is designed to reduce significant deviations from the green wave speed, facilitating the passage of traffic lights at green phases. The travel efficiency penalty r_v is formulated, as:

$$r_v = -f_v \cdot (v_{gws} - v)^2 \quad (41)$$

where f_v is the weight factor. This penalty enables the ego vehicle to track the green wave speed at signalized intersections. In addition, positive awards are introduced to alleviate the challenge of sparse rewards and incentivize the ego vehicle to drive forward. The positive awards are formulated, as:

$$r_{vpa} = f_{vpa} \frac{1}{\sqrt{2\pi}\sigma} \exp\left(-\frac{(dv - \mu)^2}{2\sigma^2}\right) \quad (42)$$

$$r_{gws} = \begin{cases} \beta_{gws}, & v_{gws_min} \leq v \leq v_{gws_max} \\ -\beta_{gws}, & v_{gws_min} \geq v \parallel v \geq v_{gws_max} \end{cases} \quad (43)$$

where r_{vpa} is the positive award, following a normal distribution to address the sparse rewards issue when the ego vehicle experiences minor velocity deviations. In addition, f_{vpa} , σ and μ are the weight factor, the standard

deviation and the mean value. r_{gws} is the positive award to encourage the ego vehicle drive forward when its velocity is within the limits of the green wave speed. Moreover, a safety reward is calculated to prevent the ego vehicle from passing traffic lights at red phases and violating speed limits. In this manner, the safety reward is formulated, as:

$$r_s = \begin{cases} -\beta_{safe}, & \text{traffic rules violated} \\ 0, & \text{otherwise} \end{cases} \quad (44)$$

where β_{safe} is the constant penalty for violating traffic rules. In this context, the reward function is ultimately formulated, as:

$$r = r_e + r_v + r_{vpa} + r_{gws} + r_s \quad (45)$$

The weight factors in above reward elements are determined through a try-and-error iterative process, and these parameters are detailed in the simulation section.

IV. SIMULATION VALIDATIONS

To validate the performance of the proposed method (called EC-DRL), simulation validations are conducted using a co-simulation platform comprising MATLAB/Simulink and SUMO [43]. The eco-driving controller and vehicle models operate in the MATLAB/Simulink environment, whereas the constructed urban scenario model is implemented in the SUMO environment. A Traci interface is utilized to realize signal interaction between the two platforms. Four benchmark strategies are selected for comparison with the proposed EC-DRL method. A rule-based strategy (SC-IDM) is constructed as the baseline benchmark, which employs lane change model LC2013 [44] to ensure travel efficiency and track green wave speed based on the IDM model [41]. The second benchmark (F-DRL) plans the ecological velocity solely based on the proposed DRL algorithm, without considering lane changes. This approach aims to simulate conventional eco-driving methods, focusing merely on optimizing longitudinal motion. The third benchmark makes lane change decisions via the LC2013 model considering travel efficiency, while optimizing ecological velocity using the same DRL algorithm. The fourth benchmark (SC-MPC) utilizes a hierarchical framework where lane change decisions are managed by the LC2013 model, and velocity optimization is carried out using MPC [5]. To ensure a desired traffic environment, the ego vehicle is scheduled to depart at the 120th second of the simulation. Additionally, the initial SOC is set to 0.32 to enable the engine to propel the vehicle.

The initial speed is set to zero, and the initial lane is set to the second lane. The basic parameters of the ego vehicle are outlined in Table 2. The parameters of the proposed method are determined through a try-and-error iterative process, and the final parameters are presented in Table 3.

Table 2. Basic parameters of the ego vehicle

Characteristic	Value
Mass (kg)	1350
Frontal area (m ²)	2.82
Air drag coefficient	0.3146
Tire rolling radius (m)	0.308
Rolling resistance coefficient	0.0135
ISG peak power (kW)	40
Engine peak power (kW)	80
Battery capacity (Ah)	40
DCT gear ratio	3.917/2.429/1.436/1.02 1/0.848/0.667

Table 3 The parameters of the proposed method

Characteristic	Value
Green wave speed factor f_{gws}	0.65
Velocity variation coefficient ξ	0.7
Transfer coefficient of travel time to driving cost ζ_t	18
Lane change penalty coefficient λ_{lc}	0.05
Lane change threshold ΔJ_c	0.1

A. DRL Parameter Setting and Training

The DRL-based velocity planner is established in the MATLAB/Simulink environment. The critic module and the actor module are constructed by two deep learning networks with multiple hidden layers of six and five, respectively. Furthermore, the neuron number in each hidden layer is set to 120. The rectified linear unit (ReLU) activation function is employed across all hidden layers, while the hyperbolic tangent (Tanh) activation function is leveraged in the output layer of the actor module. The training of DDPG agent is executed in a single-lane route environment with six signalized intersections, where the positions of traffic lights are randomized to differ from simulation tests. The maximum training episode is set to 600, with a sampling time of 0.1 s. In each episode, the initial parameters of the environment are randomized to enhance the adaptivity of the agent to various traffic conditions, including variations in SPaT information and the initial velocity of ego vehicle. The key hyperparameters for the DDPG algorithm and the reward function are presented in Table 4. The training results are shown in Fig. 5, and it can be found that the average reward gradually converges after about 180 training episodes.

Upon convergence, the agent achieves a preferable reward, thereby furnishing a trained velocity planner for online ecological velocity optimization.

Table 4. Hyperparameters for the DDPG algorithm and the reward function

Parameters	Value
Learning rate of critic network	2.00e-3
Learning rate of action network	3.00e-4
Target smooth factor	1.00e-3
Minibatch size	268
Discount factor	0.95
The weight of energy consumption f_e	16
The weight of acceleration penalty f_a	0.2
The weight of velocity deviation penalty f_v	0.025
The weight of velocity deviation penalty f_{vpa}	4
The positive reward for velocity β_{gws}	0.8
The penalty for safety reward β_{safe}	1000

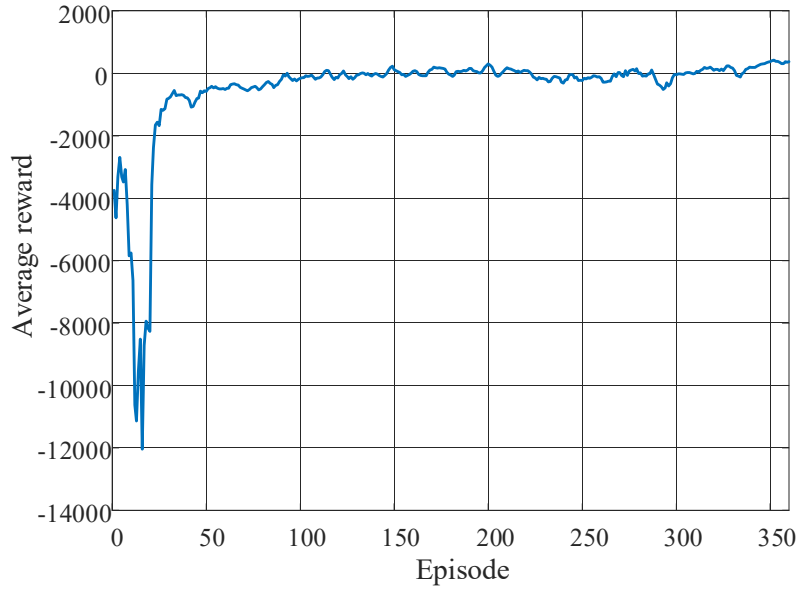


Fig. 5. Convergence of training.

B. Performance Evaluation of the Energy Economy

To sufficiently validate the energy economy of the proposed method, four driving strategies are simulated for comparison. The traffic flow is set to 400 veh/h to simulate a medium traffic condition, with several SMVs departing randomly to introduce the traffic uncertainties. The position profiles of the different strategies are illustrated in Fig. 6. It can be observed that all five methods successfully navigate the six intersections at green phases with the assistance of SPaT information. Moreover, the proposed EC-DRL method exhibits slower driving compared to the

methods which employ LC2013 lane change model. The reason is that the latter tend to make lane change decision to superior travel efficiency. However, the total travel time of the EC-DRL method shows a tiny difference in methods employing a travel efficiency priority lane change strategy, with an average difference of 1.26%. By contrast, the F-DRL method, which adheres to a fixed lane, experiences disruptions from SMVs, leading to a significant increase in travel time.

The velocity and acceleration profiles are depicted in Fig. 7. The proposed EC-DRL method pursues higher and smoother speeds compared to the F-DRL method, as illustrated in Fig. 7 (a). Specifically, the fixed-lane F-DRL method is influenced by SMVs during the simulation time from 320 s to 380 s, and the velocity is notably fluctuated and decreased. Similarly, the SC-MPC method exhibits more speed fluctuations than the proposed method, including a speed drop at 380 s, which leads to increased energy consumption. Conversely, the SC-IDM method tends to secure higher speeds to promote travel efficiency. Fig. 7 (b) shows that the DRL-based controller generates moderate acceleration decisions to reduce energy consumption. Furthermore, benefiting from predicting driving costs in candidate lanes, the fluctuations in acceleration are effectively suppressed compared to other methods. The lateral position profiles of different methods are shown in Fig. 8. The proposed EC-DRL method takes into account of both energy economy and travel efficiency, promoting the ego vehicle to transition to the third lane to improve the comprehensive performance. Notably, the frequent lane change behaviors are significantly reduced, with only one lane change operation occurring at 380 s, let alone the SC-DRL method and the SC-IDM method.

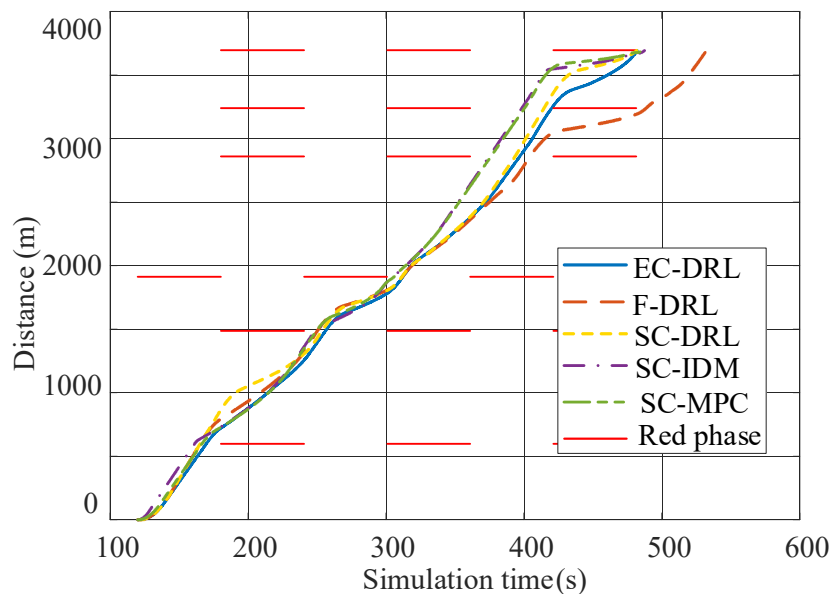


Fig. 6. Position profiles of different methods when the traffic flow is 400 veh/h

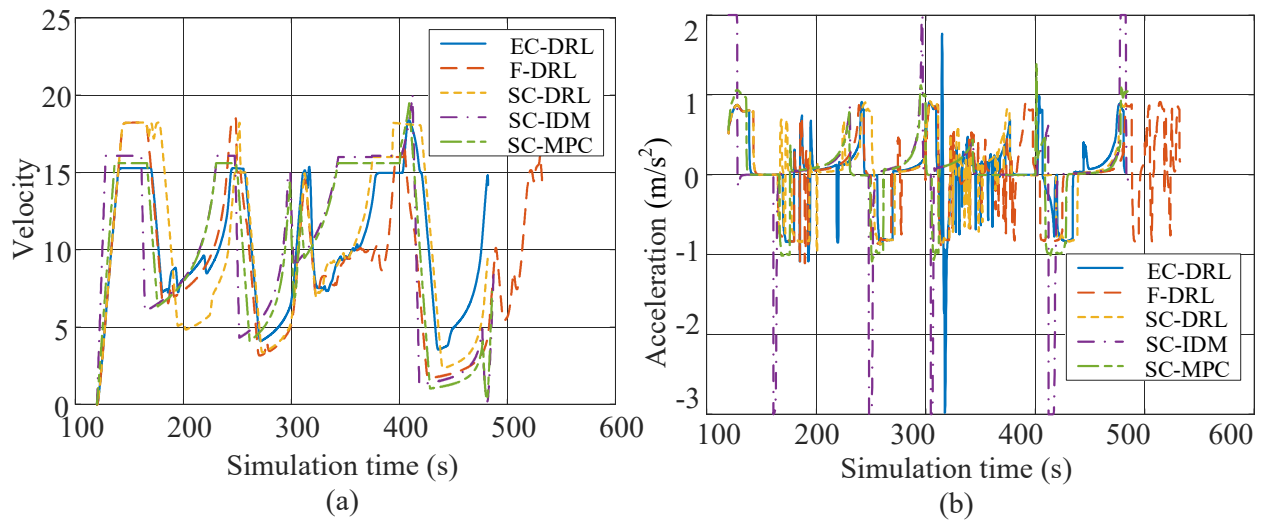


Fig. 7. Velocity and acceleration profiles when the traffic flow is 400 veh/h. (a) Velocity profiles, (b) Acceleration profiles.

Fig. 9 presents the simulation results of the powertrain system. In Fig. 9 (a), all the methods reduce the SOC to the lower limit at the destination, indicating similar levels of electricity consumption, thus the energy economy improvement primarily stems from the reduction of fuel consumption. Moreover, the SC-IDM method tends to switch to a free lane to promote travel efficiency, resulting a more rapid decrease tendency in SOC. Fig. 9 (b) illustrates the torque profiles, revealing that the proposed EC-DRL method reduces the engine operation, thanks to the optimized velocity and driving lane selection. Given that all the strategies employ the same basic energy management algorithm, the engine torque across different strategies remains similar. In other words, the enhancements in energy economy for PHEV primarily stem from ecological motion planning and reduction in engine involvement.

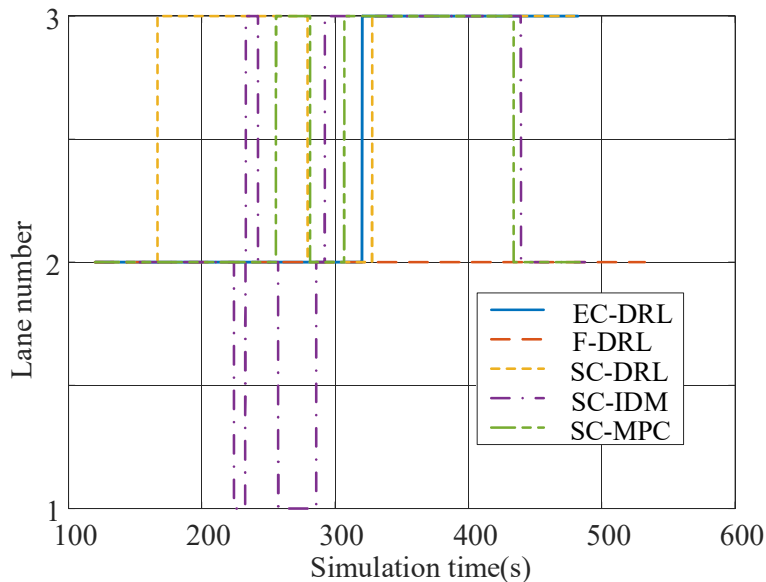


Fig. 8. Lane number of different methods when the traffic flow is 400 veh/h.

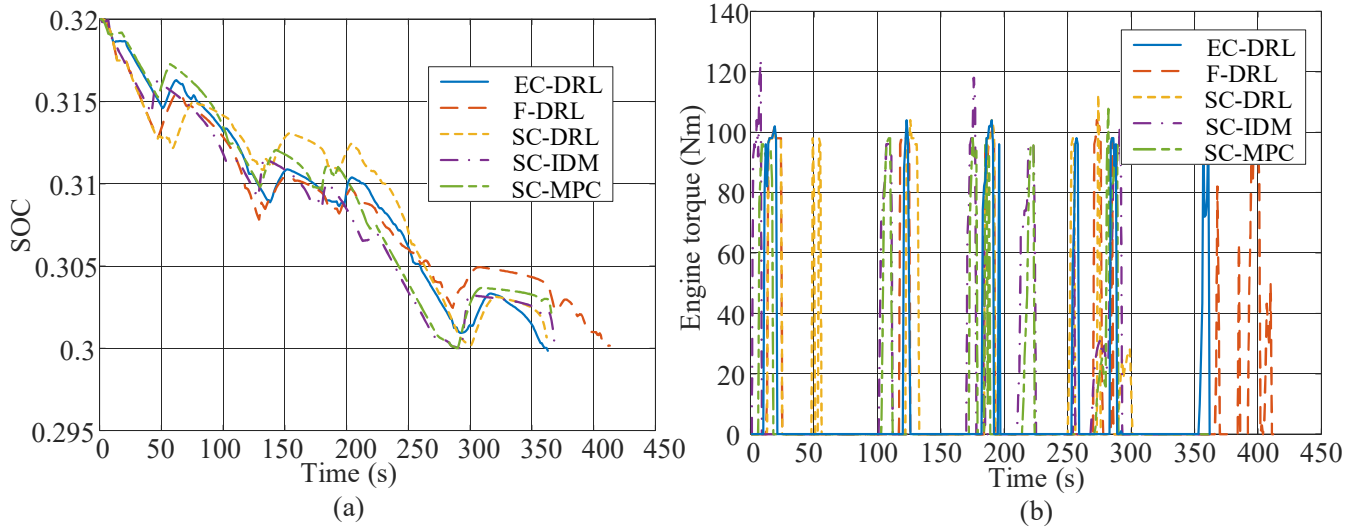


Fig. 9. Powertrain simulation results of different methods when the traffic flow is 400 veh/h. (a) SOC profiles, (b) Engine torque profiles.

The performance comparison of various strategies is summarized in Table 5. As can be found, the proposed EC-DRL method reduces energy consumption cost by 18.18%, compared to the baseline SC-IDM method, and it achieves an average energy consumption reduction of 7.18%, compared to the other three eco-driving approaches. Furthermore, the travel time of the EC-DRL method is 362.2 s, which is similar to the methods employing travel efficiency priority lane change strategy. It is worth noting that the fixed-lane F-DRL method deteriorates the energy economy and travel efficiency, compared to the proposed method, indicating the ecological lane change strategy significantly promotes the performance of eco-driving. Finally, the EC-DRL method also attains the optimality in comprehensive driving cost compared with other approaches, with a reduction of 15.31%. In summary, the proposed EC-DRL method effectively realizes eco-driving in urban scenarios by integrating lane change decisions and velocity planning, thereby comprehensively improving energy economy and travel efficiency.

Table 5. Performance comparison of different eco-driving control strategies

Approach	Energy consumption cost (CNY)	Travel time (s)	Comprehensive driving cost (CNY)	Energy consumption reduction (%)	Travel time reduction (%)	Comprehensive cost reduction (%)
SC-IDM	0.88	367.4	1.06	-	-	-
F-DRL	0.81	412.3	1.02	7.95	-12.22	4.50
SC-MPC	0.76	366.0	0.94	13.64	0.38	11.32
SC-DRL	0.79	361.8	0.97	10.23	1.52	8.75
EC-DRL	0.72	362.2	0.90	18.18	1.42	15.31

C. Verification of Adaptivity to Various Traffic Conditions

To further assess the performance and adaptivity of the proposed method in various traffic conditions, 800 individual simulation tests are conducted with different traffic flows, ranging from 200 veh/h to 800 veh/h. The SPaT information and SMVs are randomized in each case. The average variations in performance under different

traffic flows are shown in Fig. 10. The reductions in energy consumption and comprehensive driving costs are effectively achieved across various traffic flows, although the degree of reduction diminishes with increasing traffic flow. Notably, the travel time is reduced when the traffic flow is below 400 veh/h, indicating that the travel time is influenced by traffic congestions. The simulation results under free-flow and congestion conditions are then analyzed in-depth in two specific cases, with the traffic flow of 200 veh/h and 800 veh/h, respectively.

The position profiles of various methods and the lane change illustrations of the proposed method are shown in Fig. 11. As depicted in Fig. 11 (a), the ego vehicle is rarely affected by traffic uncertainties, resulting in similar position profiles among various approaches (except the F-DRL method). Fig. 11 (b) shows that the proposed method proactively transitions to the third lane to avoid potential influence from preceding SMVs in the other two lanes. Fig. 12 illustrates the results of velocity and lateral position. As depicted in Fig. 12 (a), the proposed strategy exhibits a smooth speed curve with minimal fluctuations, indicating effective ecological velocity planning by the DRL-based speed planning module. In contrast, the F-DRL strategy maintains a fixed lane position, whereas its velocity is impacted by SMVs between 320 s and 370 s, resulting in lower speeds and notable fluctuations. Fig. 12 (b) illustrates the proposed strategy executing a lane change, transitioning to the third lane at 256 s to circumvent SMVs ahead. Furthermore, the methods prioritizing speed in lane change decisions exhibit more frequent lane changes, indirectly deteriorating both energy economy and driving comfort.

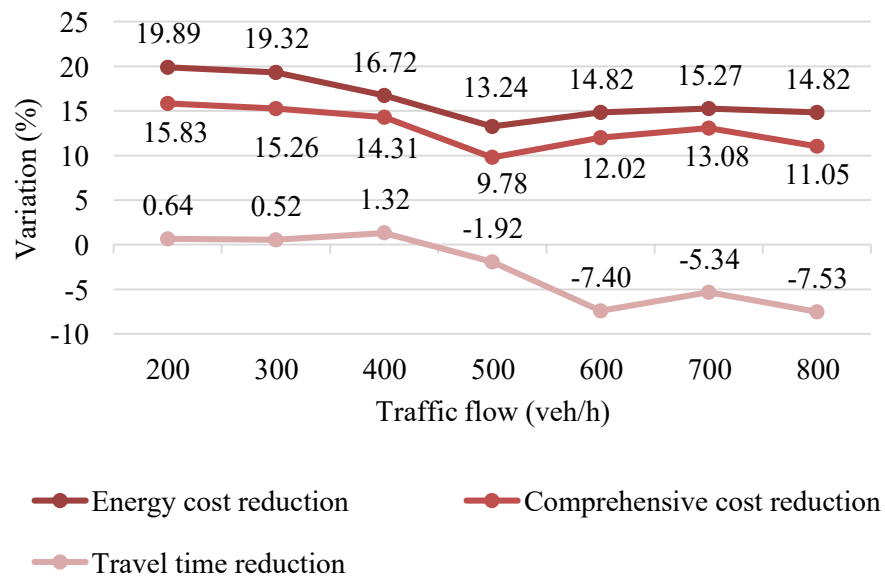


Fig. 10. Performance comparison under different traffic flow.

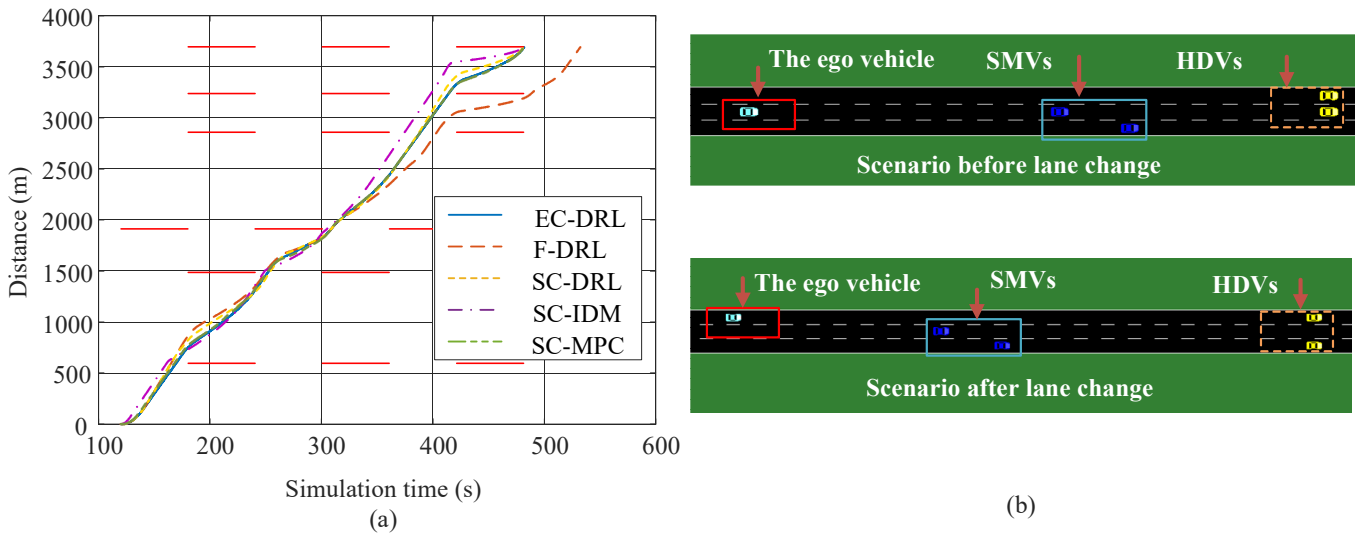


Fig. 11. Position profiles and lane change scenarios when the traffic flow is 200 veh/h. (a) Position profiles, (b) Illustrations of lane change.

The performance comparison under the free traffic condition is summarized in Table 6. The proposed EC-DRL method achieve optimality in both comprehensive driving cost and energy consumption among all benchmarks, with the maximum reduction of 20.45% and 17.04%, respectively. Additionally, compared to the SC-IDM, SC-MPC and SC-DRL strategies, which prioritize speed in lane change decisions, the proposed EC-DRL strategy exhibits similar travel times, with the variances of less than 1%. This indicates that the proposed strategy maintains commendable travel efficiency akin to the speed-preferred lane change strategy, while minimizing unnecessary lane changes.

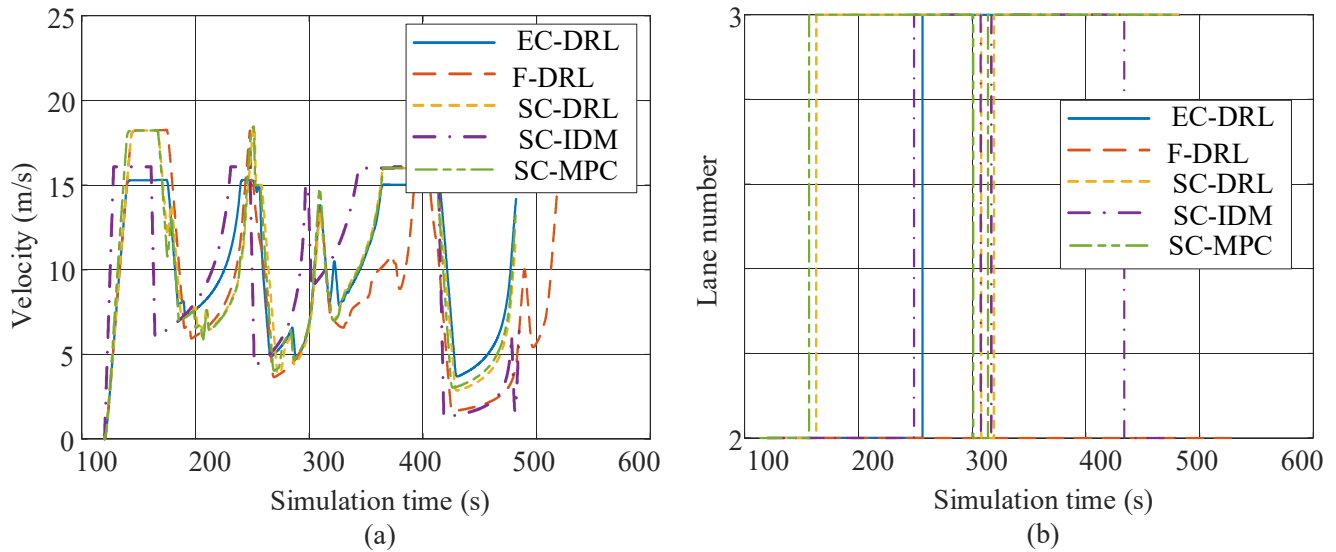


Fig. 12. Velocity and lateral position profiles when the traffic flow is 200 veh/h. (a) Velocity, (b) Lane number.

Table 6. Performance comparison when traffic flow is 200 veh/h

Approach	Energy consumption cost (CNY)	Travel time (s)	Comprehensive driving cost (CNY)	Energy consumption reduction (%)	Travel time reduction (%)	Comprehensive driving cost reduction (%)
SC-IDM	0.88	364.8	1.06	-	-	-
F-DRL	0.81	412.4	1.02	7.95	-13.05	4.31
SC-MPC	0.79	361.8	0.97	10.23	0.82	8.49
SC-DRL	0.77	361.9	0.95	12.50	0.79	10.46
EC-DRL	0.70	362.1	0.88	20.45	0.74	17.04

The position profiles and the lane change illustrations under the congestion traffic condition are shown in Fig.

13. The ego vehicle is significantly affected by SMVs, leading to a notable slowdown before the fifth intersection, and the travel time is increased, compared to the SC-IDM method. As shown in Fig. 13 (a), the proposed method maintains the same lane to ensure driving safety during congested conditions, a lane change decision is initiated only after the congestion has cleared. Fig. 14 presents the results of velocity and lateral position. It can be found that the proposed EC-DRL method leads to frequent speed fluctuations between 300 s and 400 s, due to the influence of congested traffic. Moreover, the number of lane change across various methods is remarkably reduced under the congestion traffic condition, due to driving safety constraints, as shown in Fig. 14 (b). The proposed EC-DRL method executes a lane change decision only at 410 s to avoid the influence of SMVs.

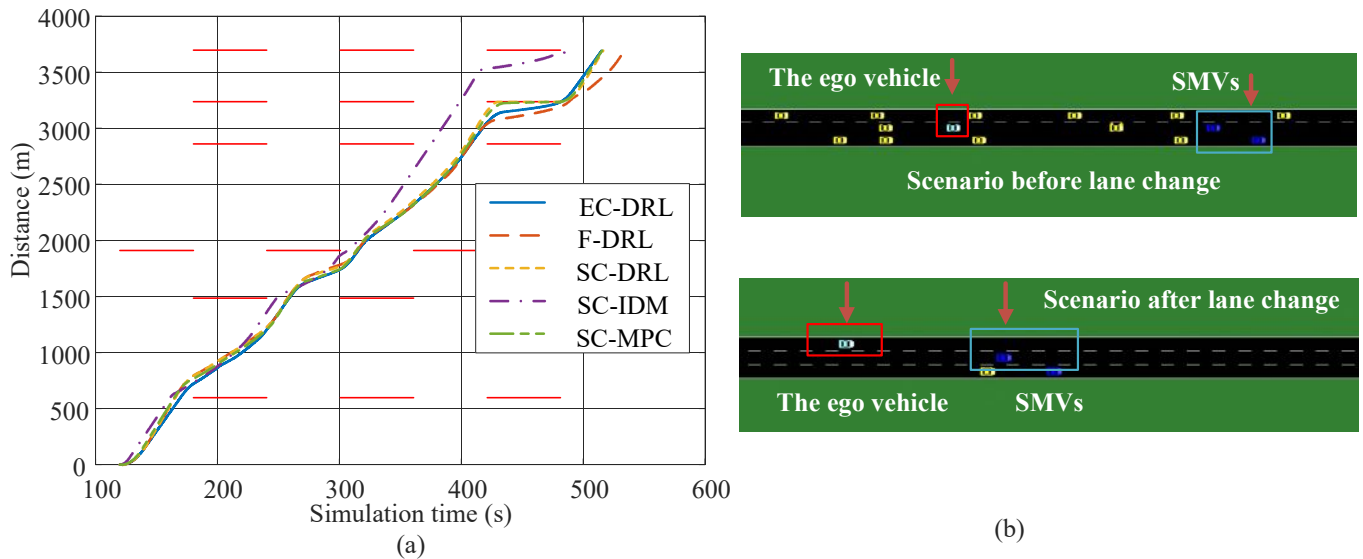


Fig. 13. Position profiles and lane change scenarios when the traffic flow is 800 veh/h. (a) Position profiles, (b) Illustrations of lane change.

The comparison results under the congestion traffic condition are summarized in Table 7. The proposed EC-DRL achieves optimal energy consumption cost, resulting in a reduction of 16.85%, compared to the basic SC-IDM strategy. However, this improvement brings the expense of a 7.68% increase in travel time. Nonetheless, the

comprehensive driving cost is reduced by 12.7%, thereby effectively enhancing energy economy and comprehensive performance. Analysis of various traffic conditions demonstrate that the proposed method effectively improves the comprehensive performance and energy economy in both free-flow and congested environments. In addition, the energy economy and travel efficiency are simultaneously improved under free-flow traffic conditions.

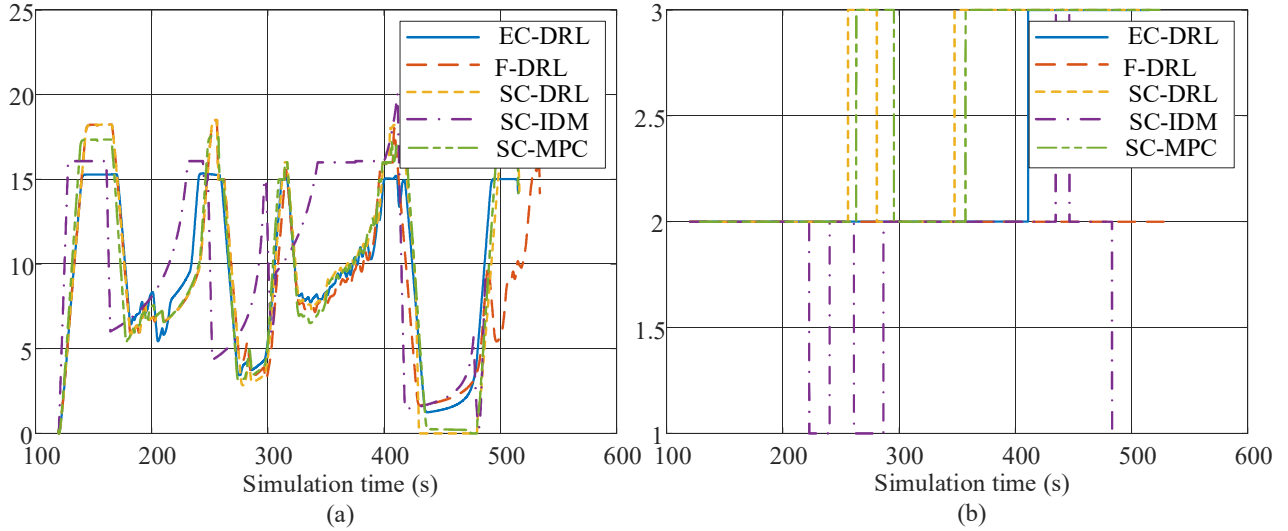


Fig. 14. Velocity and lateral position profiles when the traffic flow is 200 veh/h. (a) Velocity, (b) Lane number.

Table 7. Performance comparison when traffic flow is 800 veh/h

Approach	Energy consumption cost (CNY)	Travel time (s)	Comprehensive driving cost (CNY)	Energy consumption reduction (%)	Travel time reduction (%)	Comprehensive driving cost reduction (%)
SC-IDM	0.89	367.1	1.07	-	-	-
F-DRL	0.84	414.1	1.05	5.62	-12.81	2.51
SC-MPC	0.88	395.6	1.08	1.12	-7.76	-0.93
SC-DRL	0.94	396.5	1.14	-5.62	-8.01	-5.98
EC-DRL	0.74	395.3	0.94	16.85	-7.68	12.70

V. CONCLUSIONS

This study develops an eco-driving control strategy in urban scenarios, integrating ecological velocity planning and lane change decision-making. To preferably promote energy economy and travel efficiency, a hierarchical framework is designed to realize eco-driving, regarding the influence of SMVs and signalized intersections. In the upper layer, the energy consumption in the candidate lanes is predicted by a data-driven energy consumption model considering the influence of ecological velocity, SPaT information, preceding vehicles and traffic conditions. Furthermore, an ecological lane change strategy is developed with the comprehensive driving cost as the objective function, accounting for energy consumption and travel time. In the lower layer, the longitudinal velocity is

optimized by DRL algorithm to reduce energy consumption and travel time. Substantial simulations across various traffic conditions are conducted to validate the performance of the proposed method using a co-simulation platform. The results demonstrate that the proposed method effectively reduces comprehensive driving cost and energy consumption in all traffic conditions compared to the basic benchmark, with an average reduction of 13.05% and 16.31%. Additionally, the energy consumption and travel time are simultaneously reduced under free-flow traffic conditions.

Future work will focus on investigating the co-optimization for eco-driving and eco-routing approaches in complicated urban environments. Furthermore, the efforts should be made to establish vehicle-in-loop platform should to test eco-driving control in virtual driving environments. Approaches to enhance the computational efficiency of DRL algorithms should also be explored.

ACKNOWLEDGMENTS

This work was supported in part by the National Natural Science Foundation of China (No. 52172400 and 52272395), and in part by the project of Chongqing Automobile Collaborative Innovation Center (No. 2022CDJDX-004). Any opinions expressed in this paper are solely those of the authors and do not represent those of the sponsors.

REFERENCES

- [1] A. Vahidi and A. Sciarretta, "Energy saving potentials of connected and automated vehicles," *Transportation Research Part C: Emerging Technologies*, vol. 95, pp. 822-843, 2018.
- [2] C. Zhang, W. Huang, X. Zhou, C. Lv, and C. Sun, "Expert-demonstration-augmented reinforcement learning for lane-change-aware eco-driving traversing consecutive traffic lights," *Energy*, vol. 286, p. 129472, 2024.
- [3] X. Wei, J. Leng, C. Sun, W. Huo, Q. Ren, and F. Sun, "Co-optimization method of speed planning and energy management for fuel cell vehicles through signalized intersections," *Journal of Power Sources*, vol. 518, p. 230598, 2022.
- [4] B. Chen, S. Evangelou, and R. Lot, "Hybrid Electric Vehicle Two-step Fuel Efficiency Optimization with Decoupled Energy Management and Speed Control," *IEEE Transactions on Vehicular Technology*, 2019.
- [5] Z. Nie and H. Farzaneh, "Real-time dynamic predictive cruise control for enhancing eco-driving of electric vehicles, considering traffic constraints and signal phase and timing (SPaT) information, using artificial-neural-network-based energy consumption model," *Energy*, vol. 241, p. 122888, 2022.
- [6] J. Li, Y. Liu, Y. Zhang, Z. Lei, Z. Chen, and G. Li, "Data-driven based eco-driving control for plug-in hybrid electric vehicles," *Journal of Power Sources*, vol. 498, p. 229916, 2021.
- [7] S. Wang, K. Zhang, D. Shi, M. Li, and C. Yin, "Research on economical shifting strategy for multi-gear and multi-mode parallel plug-in HEV based on DIRECT algorithm," *Energy*, vol. 286, p. 129574, 2024.
- [8] X. Zhou, F. Sun, C. Zhang, and C. Sun, "Stochastically predictive co-optimization of the speed planning and powertrain controls for electric vehicles driving in random traffic environment safely and efficiently," *Journal of Power Sources*, vol. 528, p. 231200, 2022.
- [9] A. Bentaleb, A. El Hajjaji, A. Rabhi, A. Karama, and A. Benzaouia, "Energy-optimal control for eco-driving on curved roads," in *2022 IEEE Intelligent Vehicles Symposium (IV)*, 2022: IEEE, pp. 1584-1590.
- [10] X. Wu, J. Li, C. Su, J. Fan, and M. Xu, "A Deep Reinforcement Learning Based Hierarchical Eco-Driving Strategy for Connected and Automated HEVs," *IEEE Transactions on Vehicular Technology*, 2023.
- [11] C. Sun, J. Guanetti, F. Borrelli, and S. J. Moura, "Optimal Eco-Driving Control of Connected and Autonomous Vehicles Through Signalized Intersections," *IEEE Internet of Things Journal*, Article vol. 7, no. 5, pp. 3759-3773, 2020, Art no. 8964352.
- [12] J. Han, D. Shen, D. Karbowski, and A. Rousseau, "Leveraging multiple connected traffic light signals in an energy-efficient speed planner," *IEEE Control Systems Letters*, vol. 5, no. 6, pp. 2078-2083, 2020.
- [13] L. Guo, H. Chu, J. Ye, B. Gao, and H. Chen, "Hierarchical Velocity Control Considering Traffic Signal Timings for Connected Vehicles," *IEEE Transactions on Intelligent Vehicles*, 2022.

- [14] D. Shi, H. Xu, S. Wang, J. Hu, L. Chen, and C. Yin, "Deep reinforcement learning based adaptive energy management for plug-in hybrid electric vehicle with double deep Q-network," *Energy*, vol. 305, p. 132402, 2024.
- [15] M. Wegener, L. Koch, M. Eisenbarth, and J. Andert, "Automated eco-driving in urban scenarios using deep reinforcement learning," *Transportation research part C: emerging technologies*, vol. 126, p. 102967, 2021.
- [16] J. Li, X. Wu, M. Xu, and Y. Liu, "Deep reinforcement learning and reward shaping based eco-driving control for automated HEVs among signalized intersections," *Energy*, vol. 251, p. 123924, 2022.
- [17] Z. Bai, P. Hao, W. Shangguan, B. Cai, and M. J. Barth, "Hybrid Reinforcement Learning-Based Eco-Driving Strategy for Connected and Automated Vehicles at Signalized Intersections," *IEEE Transactions on Intelligent Transportation Systems*, 2022.
- [18] C. Zhai *et al.*, "Ecological driving for connected and automated vehicles at unsaturated intersections considering queue effects," *IEEE Transactions on Vehicular Technology*, vol. 71, no. 12, pp. 12552-12563, 2022.
- [19] Z. Yao, Y. Jin, H. Jiang, L. Hu, and Y. Jiang, "CTM-based traffic signal optimization of mixed traffic flow with connected automated vehicles and human-driven vehicles," *Physica A: Statistical Mechanics and its Applications*, vol. 603, p. 127708, 2022.
- [20] S. Dong, H. Chen, B. Gao, L. Guo, and Q. Liu, "Hierarchical energy-efficient control for CAVs at multiple signalized intersections considering queue effects," *IEEE Transactions on Intelligent Transportation Systems*, 2021.
- [21] C. Sun, C. Zhang, H. Yu, W. Liang, Q. Ren, and J. Li, "An Eco-driving Approach with Flow Uncertainty Tolerance for Connected Vehicles against Waiting Queue Dynamics on Arterial Roads," *IEEE Transactions on Industrial Informatics*, 2021.
- [22] H. Dong *et al.*, "A comparative study of energy-efficient driving strategy for connected internal combustion engine and electric vehicles at signalized intersections," *Applied Energy*, vol. 310, p. 118524, 2022.
- [23] J. Liu, C. Wang, and W. Zhao, "An eco-driving strategy for autonomous electric vehicles crossing continuous speed-limit signalized intersections," *Energy*, p. 130829, 2024.
- [24] H. Dong, W. Zhuang, B. Chen, G. Yin, and Y. Wang, "Enhanced eco-approach control of connected electric vehicles at signalized intersection with queue discharge prediction," *IEEE Transactions on Vehicular Technology*, vol. 70, no. 6, pp. 5457-5469, 2021.
- [25] W. Wang, T. Qie, C. Yang, W. Liu, C. Xiang, and K. Huang, "An intelligent lane-changing behavior prediction and decision-making strategy for an autonomous vehicle," *IEEE transactions on industrial electronics*, vol. 69, no. 3, pp. 2927-2937, 2021.
- [26] H. Yao and X. Li, "Lane-change-aware connected automated vehicle trajectory optimization at a signalized intersection with multi-lane roads," *Transportation research part C: emerging technologies*, vol. 129, p. 103182, 2021.
- [27] J. Liu, W. Zhao, and C. Xu, "An efficient on-ramp merging strategy for connected and automated vehicles in multi-lane traffic," *IEEE Transactions on Intelligent Transportation Systems*, vol. 23, no. 6, pp. 5056-5067, 2021.
- [28] S. Aoki, L. E. Jan, J. Zhao, A. Bhat, C.-F. Chang, and R. R. Rajkumar, "Multicruise: eco-lane selection strategy with eco-cruise control for connected and automated vehicles," in *2021 IEEE Intelligent Vehicles Symposium (IV)*, 2021: IEEE, pp. 302-308.
- [29] H. Dong *et al.*, "Flexible eco-cruising strategy for connected and automated vehicles with efficient driving lane planning and speed optimization," *IEEE Transactions on Transportation Electrification*, 2023.
- [30] S. Wang and X. Lin, "Eco-driving control of connected and automated hybrid vehicles in mixed driving scenarios," *Applied Energy*, Article vol. 271, 2020, Art no. 115233.
- [31] Z. Gu *et al.*, "Integrated eco-driving automation of intelligent vehicles in multi-lane scenario via model-accelerated reinforcement learning," *Transportation Research Part C: Emerging Technologies*, vol. 144, p. 103863, 2022.
- [32] H. Dong, W. Zhuang, G. Wu, Z. Li, G. Yin, and Z. Song, "Overtaking-Enabled Eco-Approach Control at Signalized Intersections for Connected and Automated Vehicles," *IEEE Transactions on Intelligent Transportation Systems*, 2023.
- [33] A. Kusari *et al.*, "Enhancing SUMO simulator for simulation based testing and validation of autonomous vehicles," in *2022 IEEE Intelligent Vehicles Symposium (IV)*, 2022: IEEE, pp. 829-835.
- [34] C. Zhai, F. Luo, and Y. Liu, "A novel predictive energy management strategy for electric vehicles based on velocity prediction," *IEEE Transactions on Vehicular Technology*, vol. 69, no. 11, pp. 12559-12569, 2020.
- [35] J. James, C. Markos, and S. Zhang, "Long-term urban traffic speed prediction with deep learning on graphs," *IEEE Transactions on Intelligent Transportation Systems*, vol. 23, no. 7, pp. 7359-7370, 2021.
- [36] H. X. Liu, X. Wu, W. Ma, and H. Hu, "Real-time queue length estimation for congested signalized intersections," *Transportation research part C: emerging technologies*, vol. 17, no. 4, pp. 412-427, 2009.
- [37] G. Padilla, C. Pelosi, C. J. Beckers, and M. Donkers, "Eco-driving for energy efficient cornering of electric vehicles in urban scenarios," *IFAC-PapersOnLine*, vol. 53, no. 2, pp. 13816-13821, 2020.
- [38] A. Sciarretta and A. Vahidi, *Energy-efficient driving of road vehicles*. Springer, 2020.
- [39] A. Kesting, M. Treiber, and D. Helbing, "General lane-changing model MOBIL for car-following models," *Transportation Research Record*, vol. 1999, no. 1, pp. 86-94, 2007.
- [40] J. Zhou, H. Zheng, J. Wang, Y. Wang, B. Zhang, and Q. Shao, "Multiobjective optimization of lane-changing strategy for intelligent vehicles in complex driving environments," *IEEE transactions on vehicular technology*, vol. 69, no. 2, pp. 1291-1308, 2019.
- [41] J. Li, A. Fotouhi, W. Pan, Y. Liu, Y. Zhang, and Z. Chen, "Deep reinforcement learning-based eco-driving control for connected electric vehicles at signalized intersections considering traffic uncertainties," *Energy*, vol. 279, p. 128139, 2023.
- [42] J. Li *et al.*, "Cooperative Ecological Adaptive Cruise Control for Plug-in Hybrid Electric Vehicle Based on Approximate Dynamic Programming," *IEEE Transactions on Vehicular Technology*, 2022.
- [43] A. F. Acosta, J. E. Espinosa, and J. Espinosa, "TraCI4Matlab: Enabling the integration of the SUMO road traffic simulator and Matlab® through a software re-engineering process," in *Modeling Mobility with Open Data: 2nd SUMO Conference 2014 Berlin, Germany, May 15-16, 2014*, 2015: Springer, pp. 155-170.
- [44] J. Dong, S. Chen, Y. Li, R. Du, A. Steinfeld, and S. Labi, "Space-weighted information fusion using deep reinforcement learning: The context of tactical control of lane-changing autonomous vehicles and connectivity range assessment," *Transportation Research Part C: Emerging Technologies*, vol. 128, p. 103192, 2021.

Eco-driving control for connected plug-in hybrid electric vehicles in urban scenarios with enhanced lane change engagement

Li, Jie

2024-11-30

Attribution 4.0 International

Li J, Liu Y, Cheng J, et al., (2024) Eco-driving control for connected plug-in hybrid electric vehicles in urban scenarios with enhanced lane change engagement. *Energy*, Volume 310, November 2024, Article number 133294

<https://doi.org/10.1016/j.energy.2024.133294>

Downloaded from CERES Research Repository, Cranfield University